Activity of Creatine Kinase in a Contracting Mammalian Muscle of Uniform Fiber Type

Eric W. McFarland,* Martin J. Kushmerick,‡ and Timothy S. Moerland§

*Department of Chemical Engineering, University of California at Santa Barbara, Santa Barbara, California 93106; ‡Departments of Radiology, Physiology and Biophysics, University of Washington, Seattle, Washington 98195; §Department of Biological Science, Florida State University, Tallahassee, Florida USA 32306

ABSTRACT We investigated whether the creatine kinase-catalyzed phosphate exchange between PCr and γATP in vivo equilibrated with cellular substrates and products as predicted by in vitro kinetic properties of the enzyme, or was a function of ATPase activity as predicted by obligatory "creatine phosphate shuttle" concepts. A transient NMR spin-transfer method was developed, tested, and applied to resting and stimulated ex vivo muscle, the soleus, which is a cellularly homogeneous slow-twitch mammalian muscle, to measure creatine kinase kinetics. The forward and reverse unidirectional CK fluxes were equal, being 1.6 $mM \cdot s^{-1}$ in unstimulated muscle at 22°C, and 2.7 $mM \cdot s^{-1}$ at 30°C. The CK fluxes did not differ during steady-state stimulation conditions giving a 10-fold range of ATPase rates in which the ATP/PCr ratio increased from approximately 0.3 to 1.6. The observed kinetic behavior of CK activity in the muscle was that expected from the enzyme in vitro in a homogeneous solution only if account was taken of inhibition by an anion-stabilized quaternary dead-end enzyme complex: E·Cr·MgADP·anion. The CK fluxes in soleus were not a function of ATPase activity as predicted by obligatory phosphocreatine shuttle models for cellular energetics.

INTRODUCTION

The only reaction catalyzed by creatine kinase is the reversible exchange:

$$PCr^- + MgADP^- + H^+ \leftrightarrow MgATP^- + Cr \quad (1)$$

The most established role for the creatine kinase (CK) reaction in muscle and other tissues is that PCr provides a buffer, or capacitance, for chemical potential of ATP during contraction that minimizes changes in the concentrations of ATP and especially of ADP during periods of increased ATPase activity (Funk et al., 1990; Meyer, 1989; Meyer et al., 1984). This role for creatine kinase is clearly demonstrated during transitions to high rates of ATP-splitting caused by muscle stimulation when the high ATPase rate sets a demand that temporarily exceeds the supply by oxidative and glycolytic ATP synthesis rates. Under these normal physiological conditions, significant change in the level of ATP does not occur but the levels of PCr and Cr (in the millimolar range) and ADP (in the micromolar range) do vary as predicted by Eq. 1. Enzyme assays of tissue extracts and ^{31}P-NMR measurements of CK chemical exchange in fast-twitch muscle and beating rat hearts have shown that this flux is at least several times the rate of ATP utilization (Meyer et al., 1982; Ugurbil, 1985; Ugurbil et al., 1986). ^{31}P-NMR measurements of CK forward and reverse fluxes in brain, heart, and skeletal muscle were explained by in vitro enzyme kinetics (Bittl et al., 1987); only resting or basal metabolic conditions were studied. A quantitative analysis of CK function in which the substrates and products of the CK reaction are maintained near equilibrium by facilitated diffusion has been presented (Meyer et al., 1984). A corollary of this model is that the fluxes catalyzed by CK should be predictable from the cellular substrate and product concentrations and the kinetic constants measured with purified enzyme in vitro. A test of the predictions of this corollary is one of the goals of these experiments.

Other interpretations of CK function were suggested by several previous investigations, including studies of respiratory control of isolated cardiac mitochondria by creatine (Jacobus, 1985; Moreadith and Jacobus, 1982; Saks et al., 1975), of the subcellular distribution of CK isoenzymes (Hoerter et al., 1988; Schlegel et al., 1988), and some reports of unequal unidirectional CK fluxes or NMR-invisible ATP pools (Bittl and Ingwall, 1985, 1987; Nunnally and Hollis, 1979; Zahler et al., 1987). In addition to these biochemical and NMR spectroscopic strategies, isotope tracers (^{18}O water and subsequent incorporation into phosphoryl moieties) are another approach that provided evidence for compartmentalization of adenine nucleotides in rat diaphragm (Zeleznikar and Goldberg, 1991). This body of work suggests that the substrates and products of creatine kinase and other relevant bioenergetic reactions (PCr, Cr, ATP, and ADP) are primarily organized and separated in organelles or in other less well-defined compartments. In that conception, the key function of the CK reaction, in the several locations in which it is found in addition to the cytoplasm, is to form essential transport links between these intracellular sites, e.g., between ATP synthesis in mitochondria and its splitting in the myofibril. This transport function with significant compartmentalization is thought to be a general property of cells containing creatine kinase (Wallimann et al., 1992) and has been termed the "creatine phosphate shuttle" (Bessman and Geiger, 1981).

Received for publication 21 May 1994 and in final form 1 August 1994.

Address reprint requests to M. J. Kushmerick, University of Washington, SB05, Seattle, WA 98195; Tel.: 206 543 3762, 3037; Fax: 206 543 3095; E-mail: kushmeri@u.washington.edu.

0006-3495/94/11/1912/13 $2.00

Several variants of the PCr shuttle concept have been described (Bessman and Geiger, 1981; Jacobus, 1980; Saks et al., 1975; Wallimann et al., 1992). A necessary property of all PCr shuttle models is that the CK flux in a steady-state rate of oxidative phosphorylation must be a direct function of the total ATPase activity. This property is a consequence of the proposed compartmentalization of metabolites and of the mechanistically necessary role that PCr is postulated to play in the intercompartmental transport; see for example Aliev and Saks (1993) and Fig. 1.5 in Jacobus (1980). This prediction is conceptually and mechanistically distinct from the co-transport of creatine, PCr, ATP, and ADP which occurs as consequence of concurrent and parallel fluxes in coupled near-equilibrium systems (Meyer et al., 1984). In that model, cellular fluxes are dominated by PCr and Cr because their concentrations are much larger than those of ATP and ADP and because of their slightly greater diffusivity. Although there is a proportionality between the CK flux and the ATP flux in obligatory shuttle models, in the facilitated diffusion model, CK flux is defined only by its substrate and product concentrations and the kinetic constants of the enzyme. We designed our experimental strategy to test these different predictions.

The quantitative relation between CK flux and cellular ATPase rate can be tested directly in living tissue using well-established ^{31}P-NMR spin-transfer techniques (Alger and Shulman, 1984; Brindle and Radda, 1987; Campbell et al., 1978), but the conclusions reported are sometimes contradictory. One of the problems with divergent results of some spin-transfer analyses is that they did not fully consider all the concurrent reactions (Ugurbil, 1985; Ugurbil et al., 1986). Another issue is that in the some preparations no single set of kinetic constants could explain the data from non-working KCl-arrested hearts and those working at 60–75% of maximal work rates (McAuliffe et al., 1991). There are at least four other possible reasons to explain lack of agreement between kinetic models and function of CK in the various tissues studied: 1) the several muscle types studied may have different cellular organizations, e.g., the myocardium has significantly more mitochondrial volume and mitochondria-bound CK than skeletal muscle; 2) the diffusion distances between mitochondria and myofibril differ in different muscles; 3) many tissues are heterogeneous with respect to cell type and the macroscopic properties are not necessarily linear combinations of the components—as is likely for tissues with mixtures of fiber types such as whole rat leg (Ariano et al., 1973) and rat diaphragm muscle (Kushmerick et al., 1992b); 4) CK activity is influenced by cytoplasmic factors (other than its substrates and products) and by activators or inhibitors not currently known or measured and which could possibly be specific to cell type.

We have investigated the kinetics of creatine kinase in an ex vivo arterially perfused cat soleus muscle preparation previously described (Kushmerick et al., 1992a; Meyer et al., 1985). In addition to being viable over long experimental periods, cat soleus muscle has a unique cellular homogeneity consisting of more than 95% slow oxidative fibers (Burke et al., 1974), in contrast to most striated muscles which are composed of distributions of two or more cell types and which display different metabolic and ATPase characteristics (Crow and Kushmerick, 1982, 1983; Kushmerick et al., 1992b). Using electrical stimulation, steady-state ATPase rates (and thus rates of oxygen consumption) are readily obtained, can be maintained at a constant rate for prolonged experimental observation (Kushmerick et al., 1992a), and can be increased 10-fold above the unstimulated rate. Soleus muscle also has a mitochondrial density (~6% volume of mitochondria/volume of fiber) which is less than that of heart muscle (~20% volume of mitochondria/volume of fiber) (Hoppeler, 1990; Hoppeler et al., 1987). The larger diffusion distance from the sites of ATP production to the myofibrillar sites of utilization in skeletal muscle should emphasize the transport function of PCr in this skeletal muscle more clearly than that obtained in the myocardium (Conley et al., 1987; Meyer et al., 1984). Both skeletal muscles and cardiac muscles have cytoplasmic (MM-CK) and mitochondrial (sMi-CK) isoforms of creatine kinase (Wallimann et al., 1992); thus a PCr shuttle, as a general mechanism, should be quantitatively more apparent and thus better tested in this slow-twitch skeletal muscle than in fast-twitch skeletal or cardiac muscle.

We developed a ^{31}P-NMR transient spin-transfer technique to measure enzyme fluxes in vivo and tested its accuracy by measuring the chemical flux of the well-defined rates of carbonic acid dehydration by ^{13}C-NMR with the same spin-transfer technique. We used this transient spin-transfer method to measure the CK flux at rest and during graded steady-state levels of activity to test the following hypotheses: 1) the CK reaction is maintained in equilibrium with the cellular content of its substrates and products, both at rest and at different ATPase rates achieved by steady-state stimulation; 2) the chemical flux through the CK reaction is independent of, and at least several times higher than, the ATPase and ATP synthesis rates (the latter two must be equal in the steady state); and 3) the in vivo flux is predicted from the in vitro enzyme kinetic constants and the observed substrate and product concentrations.

MATERIALS AND METHODS

Muscle preparation

Soleus muscles (4–6 g) were removed from adult cats (2–3 kg) under deep surgical anesthesia with sodium pentobarbital (30 mg/kg i.p. for induction, with supplemental doses for maintenance), as described previously (Meyer et al., 1985). The muscle was perfused with a 15% v/v suspension of washed human red cells in Krebs-bicarbonate-Ringer solution (pH 7.3) containing 4.4% w/v bovine serum albumin, 5 mM glucose, 0.15 mM pyruvate, 30 mg/l papaverine HCl, 10 mg/ml gentamicin sulfate, and 1–4 mM lactate (from erythrocyte glycolysis) via a cannula in its nutrient artery. Venous outflow was discarded. A peristaltic pump delivered the perfusate at a flow (0.2–1.0 ml/min with the highest flow at the highest stimulation rate) which produced a perfusion pressure ranging from 40–100 torr. The perfusate was equilibrated with 95% O_2/5% CO_2 (v/v). Full details of this preparation and its properties at rest (Meyer et al., 1985) and during and after stimulation (Kushmerick et al., 1992a) have been published.

Before data collection, each muscle was allowed to reach a steady temperature and metabolic state (22 or 30°C) for ~30 min within the NMR

probe in the magnet. These steady states were defined as a constant ratio of PCr/ATP peak heights. Control spectra and magnetization transfer data (see below) were obtained under resting conditions and during steady-state stimulation. The maximum stimulation rate (120 min^{-1}) has been shown to increase the oxygen consumption rate approximately 10-fold while remaining below the maximal rate of oxidative metabolism in the soleus (Kushmerick et al., 1992a). Five preparations were studied at 30°C at rest and while stimulated up to 60 min^{-1}. Three additional preparations were studied at rest both at 22 and 30°C. One additional muscle was able to be studied at 22 and 30°C at rest and with a range of stimulation rates.

NMR probe and in vivo spectroscopy

Magnetic resonance experiments were performed with a spectrometer built at the Francis Bitter National Magnet Laboratory (Massachusetts Institute of Technology) using an 8.5-T magnet. The perfused isolated muscle was suspended inside a radio frequency (rf) coil, which was matched to 50 Ω and tuned to 146.6 MHz. The magnet field was shimmed using the water proton signal in the muscle. After shimming, the typical ^1H line width was 0.1–0.2 ppm. An aluminum rf shield covered the entire probe body. The muscle temperature was controlled by circulating humidified room air through a glass conduit containing a resistive heating element. Temperature was monitored with a copper-constantan thermocouple fastened to the base of the muscle. Electrical stimulation was delivered by using platinum foil electrodes wrapped around the insertion and origin of the mounted muscle. The connections for the thermocouple and stimulating electrodes penetrated the rf shield after being individually filtered using series inductors (100 μH) and capacitors (10,000 μF) to ground.

The rf coil was wound in a saddle configuration using 10-gauge, high purity copper Formvar-coated wire and was connected in a balanced configuration to minimize dielectric losses. The coil had length of 3 cm and a diameter of 1.3 cm. The unloaded Q of the coil was approximately 200, and with the muscle in place, the Q was typically <100. For ^{31}P, the 90° pulse width was 23–30 μs at a nominal value of 50 W.

Control spectra were obtained from 16 or 32 averaged single-pulse experiments with a 90° pulse and an interpulse delay of 12 s. The time domain signal was detected in quadrature and 1024 points digitized at 10 kHz. The digitized signal was multiplied by a matched exponential filter and zero-filled to 4096 points before Fourier transformation. Integrals of the phase-corrected spectra with flat baselines were obtained manually and used as measures of the relative metabolite concentrations.

Spectroscopic analyses

We found it convenient to express rate constants and flux data in directly measured units of the ratio of γATP to PCr signal intensities (γATP/PCr) in each muscle. This procedure avoided the added variance by normalizing the chemical quantities to muscle mass. When needed, concentrations of PCr, Pi, and ADP were calculated from the spectral integrals using data for chemically measured values of intracellular ATP (3.67 mmol/g wet wt, equivalent to 5.03 mM in cellular water) and total creatine (17.8 mmol/g wet wt, or 22.4 mM in intracellular water) (Meyer et al., 1985). It was assumed that 1 g wet wt would equal 0.73 g of intracellular water and that the metabolites were in intracellular water only.

Intracellular pH was calculated from the chemical shift of the Pi resonance with PCr as an internal reference at −2.54 ppm relative to phosphoric acid (Kushmerick et al., 1986). A calibration curve was constructed using solutions of PCr (10 mM) and Pi (10 mM) of known pH at 25°C with added KCl (140 mM) and $MgSO_4$ (1 mM). The data were fitted to a curve defined by the following equation: $pH = 6.77 - \log[(0.89 - \delta)/(\delta - 3.19)]$, where δ is the observed Pi chemical shift. This relation was used to obtain intracellular pH from the observed chemical shift of Pi in the muscle without taking account of the small temperature difference between the muscle (22 or 30°C) and calibration solutions. The ΔH for the second ionization of phosphate is −3.7 kJ/mol, so correction for 5° temperature difference changes the pK_a value by 0.05, a difference less than the error of the measurement.

NMR spin-transfer methods

The CK-catalyzed flux was measured by steady-state saturation transfer and by transient inversion transfer NMR techniques (Alger and Shulman, 1984; Brindle and Radda, 1987; Campbell et al., 1978; Degani et al., 1987; Forsen and Hoffman, 1963, 1964; McConnell, 1957; McConnell and Thompson, 1957).

Inversion transfer technique

Inversion transfer is a transient technique for measuring chemical exchange by instantaneously labeling one of two exchanging species and observing the effect on the other. We used a selective excitation sequence, originally designed to suppress unwanted water signals in proton spectroscopy (Hore, 1983), for our transient inversion transfer experiment (McFarland et al., 1988). We found that a 90°-d-90° sequence (a two-component binomial pulse, with d = 1.4 ms) was sufficient to produce a selective 180° pulse to ^{31}P nuclei resonating at the transmitter frequency without affecting adjacent ^{31}P containing species. Note that this binomial pulse sequence does not give uniform rf excitation power over the entire spectral width. The 90°-d-90° selective inversion of PCr could reliably be used to measure rate constants as high as 50 s^{-1} without allowing significant transfer during the pulse sequence as required by the initial conditions of the McConnell equations (McConnell, 1957; McConnell and Thompson, 1957). Because of the form of the excitation spectrum and because this pulse sequence was optimized for measuring the CK catalyzed PCr-γATP exchange, only the magnetization of the PCr and γATP peaks were measured for this part of the experiment. When intensities of all the components of this ^{31}P spectrum were required, we used a standard one-pulse experiment.

After the selective inversion, the second part of the pulse sequence was a variable delay period (D2) during which spin exchange occurred between the non-inverted resonance and the inverted resonance. After this delay the net Z magnetization was sampled with an ordinary 90° pulse. An interpulse delay of 12 s was allowed between the sampling 90° pulse and the beginning of the next pulse sequence for spin-relaxation to occur. This delay is sufficient for the ATP (T_1 ~1 s) and PCr (T_1 ~3 s, see Results) resonances to have negligible (<5%) saturation effects.

Thus each measurement of CK flux consisted of the following protocol. A relaxed control inversion was made with D2 = 12 s, then six spectra after selective inversions at alternating values of D2 (typically the following times were chosen: 355, 45, 360, 55, 350, 50 ms) were performed, and finally a second control. One complete data set, consisting of the eight spectra, required 32 or 64 min, depending whether 16 or 32 averages were obtained. Steady-state stability of the preparations was tested by comparing the peak heights for the first and last control spectrum obtained in each set. Data in which there was >15% change in PCr peak height between first and second control spectra were not used for analyses.

Analysis of spin life times by initial slope approximation

We noted that there is an approximately linear recovery of magnetization during the first 400 ms after the selective inversion when the changes in magnetization are dominated by the CK-catalyzed chemical exchange. This time interval was established by independent preliminary experiments and calculations of analytical expressions of the Block equations using T_1 values and apparent rate constants which approximated our measurements. We chose our first D2 time points approximately ~50 ms after the frequency-selective 180° pulse; our second D2 time points were taken ~350 ms later to provide estimates of the initial rate of Z magnetization recovery for the inverted resonance and of Z magnetization transfer to the non-inverted resonance. To our knowledge, there have been no reports of a significant nuclear Overhauser (NOE) interaction between the PCr and ATP resonances at the high B_0 field used, although heteronuclear ^1H-^{31}P NOEs are prominent at field strengths of about 1.5 T. Our own evidence for the absence of significant NOE between PCr and γATP resonance is that at 2–4°C in two muscles, there was no detectable change in PCr magnetization with selective inversion of γATP (and vice versa). Thus the measured spin-life times of

PCr and γATP resonance can be reliably interpreted as unidirectional chemical exchange catalyzed by creatine kinase. Thus the initial slopes of the measured magnetization of the exchange-coupled inverted resonance, M_a, and non-inverted resonance, M_b, were approximated immediately after selective 180° excitation by

$$\frac{dMa/dt}{M_{a\infty} - M_{ao}} = k_{a\to b} + \frac{1}{T_{1a}} \quad (2)$$

and by

$$\frac{dMb/dt}{M_{a\infty} - M_{ao}} = -k_{a\to b}. \quad (3)$$

Selective inversion of resonance M_a has the boundary conditions M_a (t = 0) = M_{ao}, and $M_a(t = \infty) = M_{a\infty}$ dM/dt is the slope of the linear least-squares fit of the measured intensities versus time. The term $M_{a\infty} - M_{ao}$ is the difference between M_a in the relaxed spectrum (D2 ~$3T_1$), and was obtained from the y intercept of the linear least-squares fit of the $M_a(t)$ magnetization as a function of D2 times. The magnitude of the inverted magnetization (M_{ao}) ranged between 0.85 and 0.98 times that of the non-inverted magnetization ($M_{a\infty}$). Note that the measurement of $k_{a\to b}$ is completely determined by the initial slope of the non-inverted resonance and is independent of spin-relaxation characteristics in the absence of chemical exchange. This is one of the main experimental advantages over the saturation-transfer method (Alger and Shulman, 1984; Brindle et al., 1987; see below). Measurement of $k_{a\to b}$ by Eq. 3 allows a measure of T_{1a} in the same experiment.

In practice we obtained the initial slopes of PCr and γATP magnetization as a function of time by a least-squares fit of the resonance peak areas versus D2 values from 40 to 360 ms. The y intercept of the plot of the inverted species versus D2 was used as M_∞ in Eqs. 2 and 3; M_0 was obtained from the average of the two D2 = 12,000 ms values. The ratio of the chemical flux to the NMR-measurable reactant concentration is defined as a pseudo-first-order rate constant, $k_{a\to b}$ for the inversion of γATP

$$k_{PCr\to\gamma ATP} = \frac{J_{PCr\to ATP}\,(mM \cdot s^{-1})}{[PCr]\,(mM)}. \quad (4)$$

A similar analysis with the center excitation frequency of the binomial pulse centered on PCr (PCr inversion) leads to measure of $k\gamma_{ATP\to PCr}$.

The random error in k was estimated from the standard error in the fit and was found to dominate the complete error expression. Analysis of the systematic error due to the linear approximation over the finite time interval showed that the error increases with larger time intervals, increases nearly linearly in k, and decreases inversely with T_1. For the chosen values of D2 (~45 to ~360 ms) and the range of k and T_1 values measured, the estimated error due to linearization (calculations not shown) underestimated the true rate by ~7%. We used a first-order correction for the systematic error from the linear fits. The values of k and T_1 from the linear initial slope determination were used as estimates of k and T_1 in the exponential form of the complete multiexponential solutions of Eqs. 2 and 3. The systematic error that occurs when the exponential solutions are linearized was calculated by subtracting the linear fit values of k and T_1 from the k' and T_1' values that would be determined if the complete multi-exponential forms (with k and T_1) were linearized. This difference was added to the linear fit values of k and T_1 to correct for linearization. Two examples of the data obtained are given in Table 1, displaying the measurement of initial slope with the least and greatest scatter in our experimental series.

TABLE 1 Observed intensities of PCr and γATP from two experiments

	Experiment 1 (unstimulated muscle)		Experiment 2 (stimulated muscle)	
D2 (ms)	Inverted peak (γATP)	Non-inverted (PCr)	Inverted peak (γATP)	Non-inverted (PCr)
50	−2.0	10.0	−4.8	6.5
55	−4.0	10.3	−6.0	6.5
60	−1.7	12.0	−5.5	5.8
340	0.6	10.0	−3.5	4.2
350	2.0	9.5	−3.5	4.0
360	0.3	6.8	−3.6	4.2

These examples, each in different muscles, illustrate the largest and smallest scatter in the data from our inversion-transfer protocol.
Regression equations: units of t are in milliseconds. Inverted peak: M_t = 0.0119t (±0.0031) − 3.19 (±0.76); Inverted peak: M_t = 0.00658t (±0.00139) − 5.67 (±0.35); Non-Inverted peak: M_t = − 0.00717t (±0.00389) + 11.23 (±0.98); Non-Inverted peak: M_t = 0.0071t (±0.00073) + 6.71 (±0.18).

Accuracy of the inversion transfer method

To test whether this inversion transfer technique accurately measured chemical flux, we used ^{13}C-NMR to study the hydration of CO_2 catalyzed by carbonic anhydrase. In aqueous solution CO_2 reacts to form HCO_3^- directly or by way of the short-lived intermediate H_2CO_3 according to the following set of reactions:

$$CO_2 + H_2O \underset{k_{13}}{\overset{k_{31}}{\rightleftarrows}} HCO_3 + H^+ \quad (5)$$
$$k_{23} \searrow \nwarrow k_{32} \qquad k_{21} \swarrow \nearrow k_{12}$$
$$H_2CO_3$$

This reaction has been studied by non-NMR techniques with consistent results (Khalifah, 1971; Sanyal and Maren, 1981). We made measurements in solutions near pH 6.5 where the concentrations of bicarbonate and carbon dioxide were approximately equal. The solutions were prepared by bubbling ^{13}C-CO_2 into 25 mM NaOH previously purged of oxygen and by rapidly sealing the tube after titration to pH 6.5 with HCl. Inversion transfer experiments were performed over the temperature range 8–55°C to achieve a wide range of chemical exchange rates. The actual pH was calculated from the measured ratios of the CO_2 and HCO_3^- resonances and the values for the equilibrium constant extrapolated from those measured at 37°C and 0°C.

The extremely long T_1 values of ^{13}C in carbon dioxide and bicarbonate (14 and 25 s, respectively) allowed D2 times up to approximately 1 s with negligible systematic error due to linear least squares fitting. In Fig. 1, an Arrhenius plot of the NMR-derived rate constant k_{31} is shown together with the linear regression line of data taken from (Sanyal and Maren, 1981), who

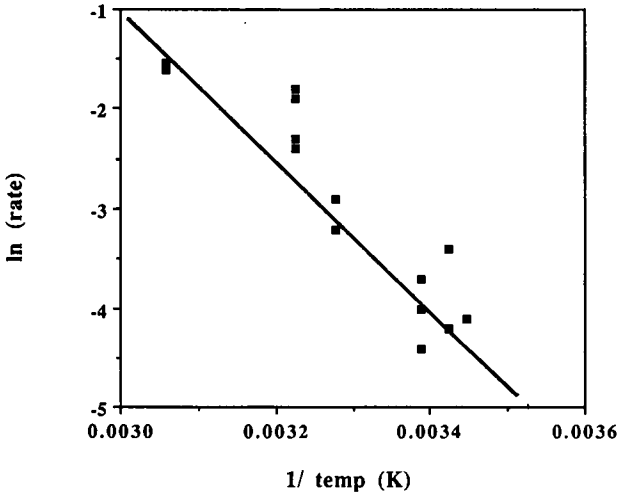

FIGURE 1 Arrhenius relationship for the hydration rate of carbon dioxide. Unidirectional rate constant, k_{31}, as defined in Eq. 5 from an inversion transfer experiment was measured as a function of temperature (■). The ordinate is the natural log of k_{31}; the abscissa is the reciprocal of the absolute temperature (°K^{-1}). The straight line is the linear regression calculated from published data obtained by independent methods (Sanyal and Maren, 1981).

used a stopped-flow spectrophotometric technique to obtain k_{31}. The activation energy of the reaction $CO_2 \rightarrow HCO_3^-$ determined from these data is 63 ± 8 kJ/mol, which is within 16% of the value of 75 kJ/mol (Sanyal and Maren, 1981). From this result we conclude that the NMR-derived rate constant obtained with a binomial-selective inversion in a transient spin-transfer experiment reflects accurately the correct rate of chemical exchange and that this model is satisfactory for a large range of k values. Note that this NMR method could give separately the values of k_{13} and k_{31} and the sum of $k_{32} + k_{31}$ and $k_{13} + k_{12}$ since a bicarbonate peak was detected, but we did not study these additional details of the mechanism of CO_2 hydration.

Saturation transfer technique

Whereas the inversion transfer experiment is analogous to a transient pulsed-label experiment, the saturation transfer experiment is a steady-state technique and thus is fundamentally different (Alger and Shulman, 1984; Brindle et al., 1987). Saturation transfer requires equilibration among the exchanging spins during a saturation pulse. A long, low power frequency-selective saturation pulse is applied to the exchanging resonances of interest, followed by a 90° readout pulse to measure its effect on the nonsaturated, exchange-coupled resonances. When chemical transfer occurs, there is a reduction in the intensity of the nonsaturated resonance from the nonsaturated value, M, to a value M_{sat}. The chemical flux can be calculated from the expression $M/M_{sat} = 1 + k \cdot T_1$, where the rate constant k for a simple two-site exchange mechanism is equal to $k_{a \rightarrow b}$ from the selective inversion method.

We used a saturation transfer method to investigate the possibility of an observable flux between γATP and Pi. The transmitter frequency was set to that of γATP and the saturation power was adjusted for complete suppression of the saturated γATP resonance in 300 ms. The measured T_1 of Pi of 4 s (Meyer et al., 1985) and an assumed $1/k$ of >6 s was used to obtain the duration of the saturation pulse ($t_{sat} = 12$ s > $[T_1 + 1/k]$). Spectra were obtained following the 12-s saturation of γATP at −5 ppm. Control spectra were obtained by setting the frequency of the 12-s saturation pulse to 0 ppm. We did not use the saturation transfer data to measure the CK fluxes quantitatively because there are several limitations of the saturation transfer technique which could preclude quantitative information from being obtained unambiguously. Several reports showed significant differences in quantitative results obtained using saturation transfer and the transient inversion transfer techniques as stated in the Introduction.

CK fluxes in in vitro solutions

CK fluxes in vitro were measured as a function of enzyme concentrations with the binomial inversion transfer method. 6000 U/ml of purified enzyme (CK from rabbit muscle, product C-3755, Sigma Chemical Co., St. Louis, MO) were added to stock solution containing 25 mM PCr, 5 mM Na-ATP, 8.3 mM KPi (added to serve as a pH reference and concentration calibration), 6 mM $MgCl_2$, 12 mM KCl, 10 mm added creatine (~0.1–0.2 mM creatine was also present as a contaminant of PCr), pH 6.8 and 1% bovine serum albumin; the solutions were mixed and equilibrated at 30°C before experimentation. The enzyme concentration was varied by sequential dilutions with stock solution. The ADP content, calculated from CK equilibrium, was 12 μM.

CK assays in soleus muscle extract

Muscles were stored on ice, minced with scissors, and ground by hand in a ground-glass homogenizer at 4°C in a solution containing 50 mM Na-PIPES (pH 7 at 20°C), 50 mM Na acetate, 4 mM DTT, 10 mM EDTA, 1 mg/ml BSA. Aliquots of the total homogenate were used to measure CK activity by a standard procedure (Sigma assay kit) at 30°C.

RESULTS

Characteristics of the NMR spectra

^{31}P spectra obtained from resting soleus at 22 and 30°C were similar in all respects to those previously reported (Kushmerick et al., 1992a; Meyer et al., 1985). The content of the ^{31}P metabolites, pH, and Gibbs free energy of resting muscle in the present experiments are listed in Table 2 and confirm previous data. At the higher temperature, there was less PCr and more Pi. The Pi line width was equal to that of the PCr resonance within ± 0.03 ppm at rest and during stimulations. This narrow line width of Pi is evidence for homogeneity of intracellular pH in the soleus muscle fibers. The concentrations of Mg^{2+} ions at 22 and 30°C were estimated to be 0.7 ± 0.3 and 2 ± 0.3 mM, respectively, from the chemical shift of the β-ATP peak by the calibrations given in (Kushmerick et al., 1986).

Steady-state electrical stimulation of the soleus caused a reduction in the PCr peak area and a corresponding increase in the Pi area. Fig. 2 shows typical spectra obtained at increasing stimulation rates. The range of steady-state stimulations studied at 30°C were accompanied by a decrease of PCr to 4 mM and a corresponding increase in Cr (calculated) and Pi (measured). For the same stimulation rate, the magnitude of the chemical changes were greater at 30°C than at 22°C (data not shown). Under steady-state conditions, the intracellular pH was unchanged, with stimulation rates as high as 90 twitches/min at both temperatures; at higher rates of stimulation, acidification occurred to pH values 6.7–6.9. During the period from rest to steady-state stimulation, there was a transient alkalinization due to the rapidly decreasing content of PCr to a new steady-state value. Transient changes were not studied in detail nor were the relationships between stimulation rates and metabolite levels because these have been reported and analyzed elsewhere (Kushmerick et al., 1992a).

TABLE 2 Summary of results in resting soleus muscle

	30°C*	22°C‡
[PCr]/[ATP]§	3.2 ± 0.6	4.0 ± 0.3
[Pi]/[ATP]§	1.7 ± 1.1	1.2 ± 0.2
pH	6.8 ± 0.1	7.0 ± 0.1
[PCr] (mM)	16.0 ± 3.0	20.0 ± 2.0
[Pi] (mM)	8.5 ± 5.5	6.0 ± 1.0
ADP¶ (μM)	15.0 ± 9.0	5.0 ± 2.0
T_1 γATP (s)	3.0 ± 0.5	1.3 ± 0.5
T_1 PCr (s)	3.8 ± 0.7	3.4 ± 0.8
T_1 Pi (s)	4.2 ± 0.3	4.4 ± 0.8
$k_{(PCr \rightarrow ATP)}$ (s^{-1})	0.17 ± 0.06	0.08 ± 0.02
$flux_{(PCr \rightarrow ATP)}$ (mM/s)	2.7 ± 1.1	1.6 ± 0.4
O_2 consumption rate‖ ($\mu mol \cdot g^{-1} \cdot min^{-1}$)	0.08	
ATPase rate** ($\mu mol \cdot g^{-1} \cdot s^{-1}$)	0.008	

* Quantities are mean ± one standard deviation for 8 muscles.
‡ Quantities are mean ± one standard deviation for 4 muscles.
§ ATP = 5.03 mM from Meyer et al., 1985.
¶ Calculated from CK equilibrium constant and total creatine (PCr + CR) content = 24.4 mM from Meyer et al., 1985.
‖ Data from Kushmerick et al., 1992a.
** ATPase rate of unstimulated muscle is estimated from O_2 consumption rate and $P/O_2 = 6.2$.

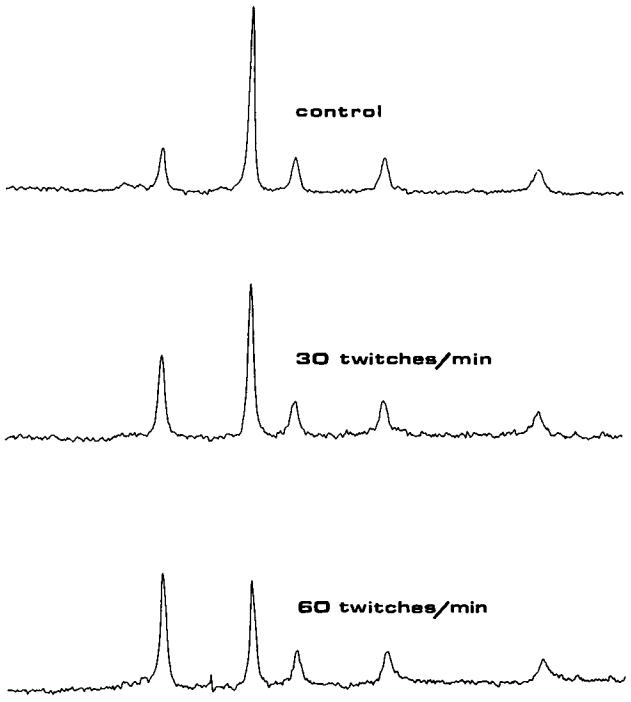

FIGURE 2 Changes in the ^{31}P spectrum during steady-state stimulation. Spectra obtained from one soleus muscle at rest (control) and at two stimulation rates: 30 twitches/min and 60 twitches/min at 30°C. From the right, the peaks are respectively: β, α, γ of ATP, PCr, Pi and minor peaks of unassigned monophosphate esters. These spectra are representative of the data obtained.

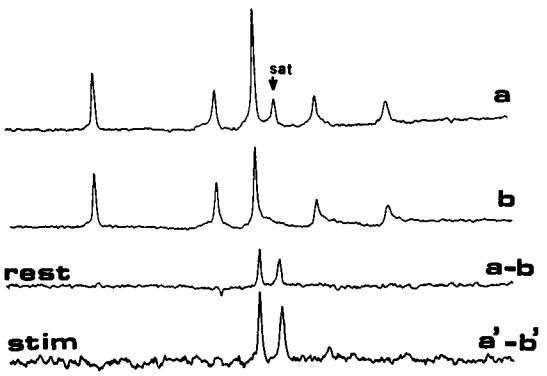

FIGURE 3 Steady-state saturation of γATP phosphate testing for ATP → Pi exchange. Control spectrum from resting soleus without saturation is shown in *a*; the locus of the saturating frequency is shown by the down arrow. The spectrum obtained after γATP saturation is shown in *b*. The spectrum obtained from same muscle by subtracting the saturated from the unsaturated data without stimulation is given in spectrum *a-b*. This difference spectrum demonstrates magnetization transfer only between PCr and γATP. Also shown is a difference spectrum of a steady-state saturation transfer experiment at 30 twitches/min; the spectrum marked *a'-b'* is this difference spectrum with the gain increased twofold from the others to emphasize the absence of exchange to Pi during the stimulation.

Tests of the validity of the two-site exchange model

The exchange between γATP and Pi is significant in heart muscle (Ugurbil, 1985; Ugurbil et al., 1986). Our experimental design for the slow-twitch soleus muscle assumed this exchange was negligible relative to the CK flux. To test the validity of this assumption, we used saturation transfer to test whether such exchange was detectable. Fig. 3 shows spectra before and after steady-state saturation of γATP. The reduction in the PCr resonance intensity demonstrates the significant γATP ↔ PCr exchange; however, no detectable transfer of magnetization was found to occur between the γATP and Pi resonances. This result excludes a significant Pi ↔ γATP exchange flux (relative to γATP ↔ PCr) under resting conditions and at 30 stimulations/min (the highest rate studied by saturation transfer). The only exchange measurable by steady-state saturation transfer was that between PCr and γATP which provides the first rationale for using a two-site exchange model for analyzing the chemical exchanges in the soleus muscle; the second justification follows.

Inversion transfer was performed to measure, singly, the bidirectional PCr ↔ γATP fluxes. The forward flux should equal the reverse if the two-site exchange model were sufficient to describe the data and if the reaction was close to equilibrium in the muscle; otherwise the model is incorrect or the reaction is not near equilibrium. Table 3 lists the results of selective inversion spin-transfer in both the forward and reverse directions in four muscles at 30°C. The mean of the ratio of the forward to reverse flux was 1.01 (± 0.08 SEM). In resting muscle the forward flux (PCr → γATP) was found to be 2.7 ± (1.1 SEM) $\mu mol \cdot g^{-1} \cdot s^{-1}$ at 30°C (Table 2). Under similar conditions (Kushmerick et al., 1992a), the resting rate of oxygen consumption was 80 nmol $O_2 \cdot min^{-1} \cdot g^{-1}$, equivalent to an ATPase rate of ~8 $nmol \cdot g^{-1} \cdot s^{-1}$. Thus it is clear that the CK flux exceeds the resting ATPase activity by two orders of magnitude. The ATPase rate measured as the steady-state rate of oxygen consumption increased about 10-fold over the range of stimulation frequencies used in the present set of experiments (Kushmerick et al., 1992a), so that the CK exchange flux, even if it changed several-fold from

TABLE 3 Balance of creatine kinase flux at 30°C

PCr/ATP	$k_{reverse}/k_{forward}$	Ratio
4.9	5.1	0.96
3.9	3.7	1.05
2.7	2.2	1.21
1.2*	1.7	0.71
2.9	2.5	1.16
3.1	3.2	0.95
		Mean 1.01 ± 0.07 (±SEM; N = 6)

$k_{forward}$ is the pseudo-first order rate constant measured in the forward direction, i.e., ATP synthesis: PCr → γATP. $k_{reverse}$ is the corresponding pseudo-first order rate constant for the reverse direction γATP → PCr. Ratio indicates the ratio of the forward flux to the reverse flux and is equal to (PCr content · $k_{forward}$)/(ATP content · $k_{reverse}$) calculated by dividing the column PCr/ATP by the column $k_{reverse}/k_{forward}$.

* stimulated at 15 twitches/min. All others measurements are from resting muscles.

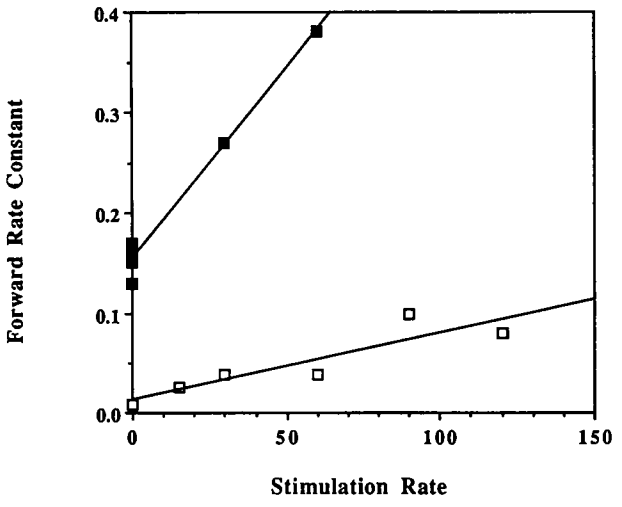

FIGURE 4 The increase in the forward rate constant, $k_{PCr\rightarrow\gamma ATP}$, with stimulation rate. The observed pseudo-first-order forward rate constant, defined in the text and Eq. 4, is displayed as a function of the twitch stimulation rate. The data were obtained in one soleus at two temperatures, up to 60 twitches/min at 30°C (■) and 120 twitches/min at 23°C (□). Ordinate unit is reciprocal seconds; abscissa is in units of twitches per minute.

its value at rest, would still be sufficient to maintain the reaction near equilibrium. CK flux in excess of ATPase and ATP synthesis rates is a necessary condition for the CK reaction to be at equilibrium with its substrates and products.

CK fluxes during steady-state period of stimulation

The content of PCr declines to a new steady state with stimulation (Kushmerick et al., 1992a). In Fig. 4, the observed apparent rate constant $k_{PCr\rightarrow\gamma ATP}$ for one muscle is plotted versus the ratio, ATP/PCr, obtained directly from the spectra. At both 22° and 30°C, $k_{PCr\rightarrow\gamma ATP}$ varies approximately linearly with ATP/PCr. The result of $k_{PCr\rightarrow\gamma ATP}$ versus ATP/PCr for all data obtained at 30°C is displayed in Fig. 5. These results show that as the content of PCr decreases, the pseudo-first order rate constant, $k_{PCr\rightarrow\gamma ATP}$, increases. The ADP concentration is implicitly included in the definition of this rate constant; see Eq. 4. This increase in magnitude of $k_{PCr\rightarrow\gamma ATP}$ can be explained by the increase in ADP, which is related to (and calculated from) the PCr content and the ATP/PCr ratio by the CK equilibrium. Except at the highest stimulation rates, the intracellular pH remained at 6.9 as also noted previously (Kushmerick et al., 1992a), thus the pH effects on this apparent rate constant are small compared to those of ADP. The temperature dependence of this apparent rate constant yields a Q_{10} of about 2.

The next result is the main test of the second hypothesis given in the Introduction: how does the steady-state forward flux catalyzed by CK reaction change with stimulation as the ATPase rate increases? The forward CK flux (PCr → γATP) was calculated from the product

$$\text{Flux} = \left(\begin{matrix}\text{ATP}\\ \text{content}\end{matrix}\right) \cdot \left(\begin{matrix}\text{observed rate}\\ \text{constant}\end{matrix}\right) \cdot \left(\frac{\text{PCr}}{\text{ATP}}\right) \text{ratio}$$

$$= 5.03 \cdot (k_{PCr\rightarrow\gamma ATP}) \cdot (\text{PCr}/\gamma\text{ATP})$$

where 5.03 is the content of ATP (μmol·g^{-1}) in perfused cat soleus muscles (Meyer et al., 1985); the units of flux are then μmol·g^{-1}·s^{-1}. The results from all preparations at 30°C are shown in Fig. 6. The least-squares slope is not significantly different from 0; the trend for the flux to decline as PCr decreases was not statistically significant. The increase in the apparent rate constant ($k_{PCr\rightarrow\gamma ATP}$) was apparently counterbalanced by the decrease in PCr content such that the forward

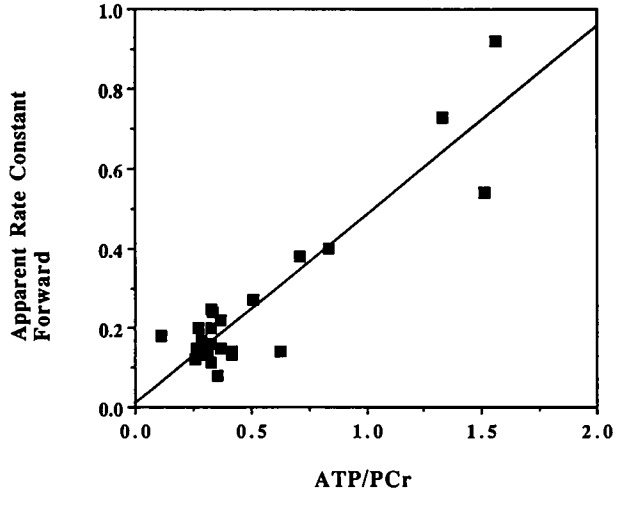

FIGURE 5 Observed forward rate constant, $k_{PCr\rightarrow\gamma ATP}$, as a function of ATP/PCr metabolite ratio. NMR derived rate constant in six soleus preparations was determined by transient selective inversion transfer in the direction: PCr → ATP. The ordinate is the observed pseudo-first-order rate constant, as in Fig. 4, defined in the text and Eq. 4. The abscissa is the ATP/PCr ratio in the muscle while the inversion transfer measurements were made. Data were obtained at rest and after graded electrical stimulation in the soleus to 60 twitches/min. Muscles were maintained at 30°C.

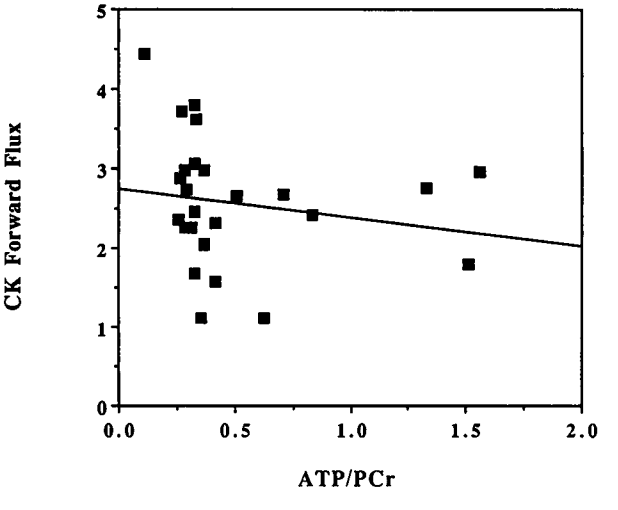

FIGURE 6 CK flux (mM·s^{-1}) as a function of the ATP/PCr ratio. Data from the same muscles as in Fig. 5. At rest the average ATP/PCr ratio was ~0.3 and increased to nearly 1.6 at stimulation rates at 60 twitches/min. Best linear least-squares fit gives a slope of −0.26 ± (0.34) mM/s, not statistically different from 0.

flux did not detectably change under conditions wherein the rate ATPase increased on the order of 10-fold. Measurements of O_2 consumption were not made in the present experiments, but other experiments have (Kushmerick et al., 1992a) quantified oxygen consumption versus stimulation rate in this preparation and have demonstrated a 10-fold increase in the same muscle at 30°C for similar stimulation rates. Since the experiments were made in the steady state, the rates of ATP synthesis balanced its utilization.

Creatine kinase assays in soleus muscle extract

Assays of CK activity were performed on extracts of the contralateral soleus from two animals on the same day as the NMR experiment. The averaged activity in fresh soleus homogenates was 1270 (range ± 25) U/g wet wt, corresponding to ~1690 U/ml intracellular water. One unit of activity is that amount of enzyme which transfers 1 μmol of phosphate from PCr to ADP per minute at the assay condition of 30°C at pH 7.4. Thus the flux under these in vitro conditions of maximal enzyme activity corresponds to a forward flux of ~28 $mM \cdot s^{-1}$, about 10 times larger than the flux in vivo (Fig. 6 and Table 2) measured by spin transfer.

Creatine kinase fluxes in vitro with enzyme solutions

The NMR-derived rate constant $k_{PCr \rightarrow \gamma ATP}$ was measured as a function of CK enzyme concentration in vitro by the inversion transfer technique. The goal was to make a second estimate of the CK activity in the soleus by comparing apparent rate constants in the muscle with that measured in solution mimicking the composition of the cytoplasm. The solutions used contained 25 mM PCr and 5 mM ATP and CK at pH 7 at concentrations of 1000–6000 U/ml at 30°C. The pseudo-first- order rate constant CK flux, $k_{PCr \rightarrow \gamma ATP}$, in this solution increased in proportion to the enzyme concentration as expected. Thus we could scale the CK activity in the muscle by noting the concentration of enzyme in solution which gave the same rate constant as measured in the muscle. Comparison of the NMR-derived rate constant in resting soleus (0.17 s^{-1}, Table 2) with the enzyme in vitro results indicates that the CK activity in resting muscle intracellular water is equivalent to approximately 3200 U/ml by this assay, or ~53 $mM \cdot s^{-1}$. The reasons for the twofold difference in the estimates of the CK activity by NMR spin transfer of the enzyme in vitro (~3200 U/ml) and by enzymatic assay of extracts (~1700 U/ml) were not established, and likely are explained by lack of complete solubilization or inactivation of enzyme during the homogenization, by differences in the ionic environment and pH of the cytoplasm and the in vitro solutions, or by other factors by which the two assay conditions differed. Thus the data from both in vitro assays place the CK activity in soleus muscle on the order of 30–50 $mM \cdot s^{-1}$ in the forward direction (PCr → γATP).

DISCUSSION

The two major results from our experiments are discussed in order. The first is that the forward and reverse CK fluxes were equal and did not increase significantly over a range of stimulation rates which increased the ATPase rate by one order of magnitude and decreased the PCr content from 17 mM to 4 mM (with corresponding changes in other metabolites). The second is that these in vivo fluxes are an order of magnitude lower than that measured by CK activity in muscle extracts and in in vitro solutions of CK mimicking the composition of the cytoplasm.

Independence of the creatine kinase fluxes with ATPase

The range of stimulation rates used was sufficient to change the ATP/PCr ratio from a value at rest of 0.3 to 1.6, corresponding to a range of PCr content of 16 $\mu mol \cdot g^{-1}$ at rest to 3 $\mu mol \cdot g^{-1}$ during high rates of stimulation. Based on a detailed study of steady-state oxygen consumption under similar conditions (Kushmerick et al., 1992a), these stimulations result in a more than 10-fold increase in the steady-state ATPase and ATP synthesis activity of the muscle caused by an increase in ADP content from ~4 $nmol \cdot g^{-1}$ at rest to >80 $nmol \cdot g^{-1}$ at high steady-state stimulation rates. The apparent rate constant ($k_{PCr \rightarrow \gamma ATP}$) did increase, and the decrease in PCr, with increasing rates of stimulation, counterbalanced the change in $k_{PCr \rightarrow \gamma ATP}$ such that actual flux (PCr content · $k_{PCr \rightarrow \gamma ATP}$) did not change.

The lack of dependence of CK flux with ATP utilization rate agrees with and extends to this muscle with a homogenous fiber type the results obtained in intact rat leg muscle using steady-state saturation transfer methods (Le Rumeur et al., 1992; Shoubridge et al., 1984), and in rat heart (Ugurbil et al., 1986). This independence of CK flux with ATP turnover rate is clearly at variance with the prediction of PCr shuttle models which require an obligate transport function for PCr coupling ATPase to CK flux. Thus our experiments demonstrate that the necessary condition of these PCr shuttle models, viz. that the CK flux is a function of the total ATPase activity of the cell, does not hold in this muscle. As we argued in the Introduction, this muscle, with its intermediate mitochondrial density and diffusion distances between mitochondria and myofibrils larger than that in the myocardium, provides a cellular organization sensitive for this test. Our results thus exclude the operation of a PCr shuttle mechanism in the slow-twitch soleus muscle as the primary and obligatory mechanism for transport of high-energy phosphate. As emphasized previously (Meyer et al., 1984), this result does not exclude a transport function for PCr; in fact, transport and buffer functions of CK activity reflect the same basic near-equilibrium mechanism.

It is possible within the errors of measurement that one or more compartments may exist and display the required properties of shuttle models and would not have been detected by the spin transfer method. Without a specific shuttle model

and an analysis of propagation of errors in it, no precise limit can be placed on the largest size of such a compartment consistent with our results. Our results show that the predominant features of cellular energetics are adequately described by near-equilibrium principles and the contribution of CK compartments can only be within the error of our experiments, i.e., ~14% of total CK flux (SEM/mean for 30°C from Table 2). Compartments containing CK substrates and products at such a small fraction of the total would not be measurable in our measurements. For example, if the mitochondrial volume contained 10% of the total cell CK substrates and products as is likely, the size of that compartment would be within the error of our experiment.

There are differences between ours and related experiments in muscle that deserve comment. Our conclusions do not agree with those of (Zahler et al., 1987) who used saturation transfer methods in rat quadriceps muscle, but there is no contradiction in data. With stimulation of the muscle, the chemical exchange rate constant was higher than at rest as consistent with our results. An enzyme kinetic scheme was not used to interpret the data. Also the interpretation of the CK kinetics and the compartments identified was entirely dependent on the NMR spin transfer model used. Further comparisons cannot be made because of the lack of information on the uniformity of the cell activation and fiber type and on the physiological range of activity of the muscle studied. The recent report (Van Deursen et al., 1993) of absent cytoplasmic isoform of creatine kinase (MM-CK) in transgenic mice showed that there was no NMR-detectable flux in the hind limb of the knockout mice, yet the muscle was capable of splitting PCr during contractile activity (1 and 5 Hz stimulation rate) indistinguishable from controls. These results mean physiologically relevant CK fluxes can occur in the apparent absence of NMR-detectable flux. At face value there is a contradiction here in that there was clearly splitting of PCr with muscle activation supposedly in the complete absence of enzyme in the cytoplasm. Since enzymatic catalysis is essential, the mitochondrial enzyme must have been active in this process either by its presence in the cytoplasm or by easy access of the metabolites to the mitochondrial space (in which case the compartmentalization of that CK isoform in the best defined intracellular compartment loses its functional meaning). It cannot be assumed that the sole change in metabolic organization of these muscles is a decrease in CK; other aspects of cellular function almost certainly have changed in the cells during the developmental history of the animals missing MM-CK. Nonetheless the muscles of these animals deserve further quantitative study for a number of reasons including the need to resolve the discrepancy between NMR measured flux and enzymatically measured activity reported. Indeed there was a measurable quantitative discrepancy in our experiments between in vitro assays and in vivo NMR assays of CK flux, discussed in the next section, which we could explain by known properties of the enzyme. Finally, in rat diaphragm (Zeleznikar and Goldberg, 1991) used isotope tracers (^{18}O water and its subsequent incorporation into phosphoryl moieties) to provide evidence for compartmentalization of inorganic phosphate and adenine nucleotides. With this technique distinguishable pools of metabolically active inorganic phosphate, ATP and other relevant metabolites were found and the magnitude of these depended on the state of contractile activity of the muscle. These data show evidence for greater complexities in the various reactions involving high-energy phosphates than do our experiments. Note that the rat diaphragm is one of the most cellularly heterogeneous muscles, containing approximately equal fractions of muscle cell types 2A, 2X, and 1. Our NMR method focused on only the exchange catalyzed by CK, and in that narrower sense there is no difference in the results, because the authors state that the data are consistent with a similar cellular distribution of PCr and ATP and equilibration by CK activity among its substrates and products (Zeleznikar and Goldberg, 1991).

In vivo CK flux is less than predicted from enzyme kinetics

The measured equality of the forward and reverse fluxes, and the absence of significant γATP → Pi transfer, are entirely predicted by a two-site exchange between PCr and γATP and by the CK reaction buffering the ATP and ADP contents. Principles of enzyme kinetics further predict that, with stimulation or another operation that alters the cellular metabolite levels, changes in CK flux will be defined by the steady-state kinetics of the enzyme under its new substrate and product concentrations. Our results showed that the pseudo-first-order rate constant increased, but the flux did not change because of counteracting decreases in PCr content. Can these observations be predicted quantitatively by the well-known properties of CK in solution?

The reaction mechanism for CK is a rapid equilibrium random (RER) mechanism in the forward direction (ATP synthesis) at neutral pH (Schimerlik and Cleland, 1973) and an equilibrium-ordered (EO) mechanism in the reverse direction, with MgATP binding before Cr. At pH 8, the reaction mechanism is bidirectionally a RER mechanism (Morrison and Cleland, 1966). The steady-state velocity expression (with the use of the terminology and reaction scheme given by Schimerlik and Cleland for pH 7 and constants from Table 4) can be written as follows:

$$\frac{\text{Reaction velocity}}{V_{max}} = \frac{N}{D} = \frac{V}{V_{max}} \tag{6}$$

where, for the forward direction measured in this paper, N is given by

$$N = \frac{[\text{MgADP}] \cdot [\text{PCr}]}{\text{Kia} \cdot \text{Kb}}. \tag{7}$$

TABLE 4 Kinetic constants used in calculating CK flux

Constant	Value (mM)
Michaelis	
Ka	0.04
Kb	1.11
Kp	3.8
Kq	0.057 (Schimerlik and Cleland define as 0)
Dissociation	
Kia	0.135
Kib	3.9
Kip	554 (Schimerlik and Cleland define as ∞)
Kiq	3.5
Inhibitory	
KIa	0.015 (Schimerlik and Cleland define as 0)
KIb	3.9
KIp	58
KIq	3.2
KIi	0.1–0.4 (anion inhibitory constant, ~1 mM in Watts (1967))

All values are adopted from Schimerlik and Cleland (1973) or Watts (1967).

D represents the terms for the relevant enzyme complexes:

$$D = 1 + \frac{[\text{MgADP}]}{\text{Kia}} + \frac{[\text{PCr}]}{\text{Kib}} + \frac{[\text{MgADP}] \cdot [\text{PCr}]}{\text{Kia} \cdot \text{Kb}} + \frac{[\text{MgATP}]}{\text{Kiq}} + \frac{[\text{Cr}] \cdot [\text{MgATP}]}{\text{Kp} \cdot \text{Kiq}}. \quad (8)$$

The expressions in Eq. 8 reflect that the CK reaction in the cell has both forward and reverse flux components. V_{max} is the maximal forward enzyme rate when all the enzyme is in the ternary complex: E · PCr · MgADP form; we estimated its value at 30–50 mM·s^{-1} from both in vitro assays described in Results. The left-hand expression of Eq. 6 is the predicted flux as a fraction of the maximal enzyme activity. Additional terms may be added to Eq. 8 to reflect the existence of dead-end ternary complexes, e.g., E · MgATP · PCr and E · MgADP · Cr.

We next tested the extent to which the published in vitro data can explain our in vivo fluxes (displayed in Fig. 6) by comparing the observed data with solutions of the kinetic equation with the substrate binding constants from Schimerlik and Cleland (1973). With the constants listed in Table 4 and the average values of substrate and product concentrations in unstimulated muscle from Table 2, we calculated the flux using the equations above by decrementing the content of PCr in steps, at each step computing a new set of ATP, ADP, and Cr values as defined by the CK equilibrium. This process was iterated over the range of ATP/PCr values measured; the results are displayed in Fig. 7. The curves represent the five sets of enzyme complexes modeled. The first predicted flux with all of the normal substrate and product complexes defined in Eq. 8 and is plotted in curve A. With addition of the E·Cr·MgADP dead-end complex the predicted flux is closely similar, curve B. This flux was calculated by adding the following term to Eq. 8:

$$\frac{[\text{Cr}] \cdot [\text{MgADP}]}{\text{KIp} \cdot \text{Kia}}$$

The addition instead of only the E·PCr·MgATP dead-end complex was modeled by adding the following term to Eq. 8:

$$\frac{[\text{PCr}] \cdot [\text{MgATP}]}{\text{KIb} \cdot \text{Kiq}}.$$

The result was a small decrease in overall flux reduction, but with no significant change in the qualitative behavior, curve C. With addition of both of these dead-end complexes, the predicted flux continued to remain essentially unchanged, curve D. All four of these calculations displayed a twofold monotonic increase in flux as PCr decreased over the range of our experimental observations (from small to large values of ATP/PCr); see also Shoubridge et al. (1984) and Kupriyanov et al. (1984), who came to a similar conclusion. Systematic increases and decreases (up to 10-fold) in the values of the constants listed in Table 4, with the appropriate detailed equilibrium balances as required by the rapid equilibrium enzyme mechanism (Morrison and Cleland, 1966) maintained the monotonic increase in flux as ATP/PCr increased. None of these trials reproduced the observed lack of change in CK flux displayed in Fig. 6.

It was possible, however, to account for the observed data by adding a term for the E · Cr · MgADP dead-end complex which takes into account the stabilization of this dead-end complex by planar anions. The flux was calculated by replacing the terms for the dead-end com-

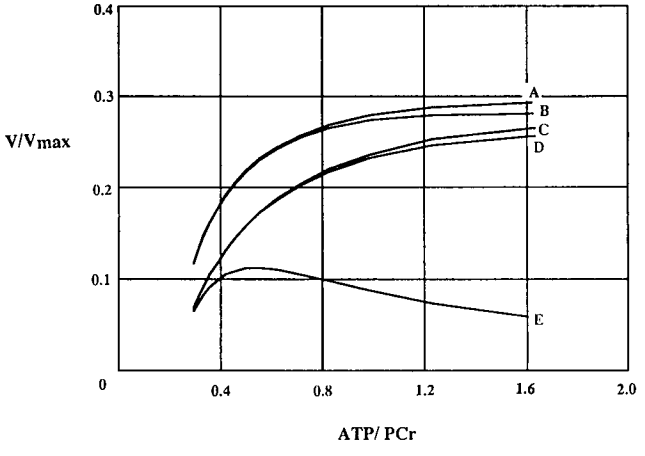

FIGURE 7 CK fluxes as predicted by a model of the enzyme reaction. The kinetic scheme defined by Eqs. 6–8 and constants measured at pH 7.0 from Table 4 were used to calculate the relative flux (V/V_{max}) as a function of ATP/PCr ratio. Metabolite concentrations from Table 1 at 30°C were used in an interactive calculation which decremented PCr while maintaining CK equilibrium. The five curves represent the addition of terms for various enzyme complexes as follows: A: the predicted flux with all of the normal substrate and product complexes considered as defined by Eq. 8; B: addition of the E · Cr · MgADP dead-end complex; C: addition of only the E · PCr · MgATP dead-end complex; D: addition of both dead-end complexes; E: normal substrate and product complexes with the addition only of the E·Cr·MgADP dead-end complex stabilized by adding a term for the planar anions with [anion] = 25 mM and KIi = 0.25 mM.

$$\frac{[\text{anion}] \cdot [\text{Cr}] \cdot [\text{MgADP}]}{\text{KIi} \cdot \text{KIp} \cdot \text{Kia}}.$$

plexes considered above with a term for a quaternary complex, E · anion · Cr · MgADP:

$$\frac{[\text{anion}] \cdot [\text{Cr}] \cdot [\text{MgADP}]}{\text{KIi} \cdot \text{KIp} \cdot \text{Kia}}$$

in Eq. 8 and the calculated flux shown by curve E in Fig. 7. Planar anions such as NO_3^-, and Cl^- and HCO_3^- (the last two of which are abundant in the cytoplasm; Cl^- about 16 mm (Dulhunty, 1977) and HCO_3^- about 10 mM (Roos, 1971) are known to stabilize the dead-end complex (Watts, 1967). Values of KIi in vitro are in the millimolar range (Watts, 1967). Intracellular [Cl^-] is a function of the membrane potential and its extracellular concentration (Dulhunty, 1977). From that data and the composition of our Krebs-bicarbonate-Ringer solution, we estimate the intracellular [Cl^-] to be 16 mM. Intracellular [HCO_3^-] is a function of cellular pH and extracellular pCO_2 (Roos, 1971). From the data of Roos, we estimate intracellular [HCO_3^-] to be 10 mM. We used values for KIi over the range of 0.1–0.4 mM and a concentration of 26 mM for the sum of [Cl^-] and [HCO_3^-] to achieve the result shown in Fig. 8, which shows that the calculated curves approximate the envelope of the observed data (Fig. 6). The detailed shape of the fluxes predicted by the equation containing the term for the inhibitory quaternary complex remains curvilinear and has a maximum, but experimental scatter makes it impossible to see this detail in the data. This agreement between the modeled and observed flux suggests that this quaternary complex is a dominant form of enzyme-substrate and enzyme-product interactions in muscle cells. Thus normally CK activity is significantly inhibited.

Hence this model of CK kinetics can account for the measured in vivo flux by several criteria. First, the major result shown in Fig. 6 is that the CK flux does not change with the stimulation-induced metabolite changes. Second, the magnitude of the observed flux in the muscle is an order of magnitude lower than that estimated in muscle homogenate or comparable amounts of CK in solution in vitro. Quantitatively the predicted fractional flux (flux/V_{max}) in the kinetic model with the anion-stabilized dead-end complex is on the order of 0.1 (curve E in Figs. 7 and 8). As discussed above, the maximal forward flux of CK (V_{max}) in these muscles was estimated to be 30–50 mM·s^{-1} showing that this ratio of observed flux (~3 mM·s^{-1}) to V_{max} (30–50 mM·s^{-1}) is ~0.1. There are apparently major effects of intracellular anions such as chloride and bicarbonate which influence the CK kinetics by the quaternary dead-end complex, E · anion · Cr · MgADP. The formation of this complex effectively binds a significant fraction of creatine kinase into a nonproductive form. This effect has been noted in vitro (Watts, 1967), and our results indicate this effect may be important in vivo as well.

Our finding that the CK chemical kinetics in the intact cell is adequately described in terms of a well-mixed solution of enzyme, substrate, and products with respect to the exchange and diffusion of PCr, Cr, MgATP, and MgADP suggests a model wherein MM-CK has apparently equal access to one common pool of substrates and products, despite the clear evidence for its distribution in cytoplasmic and myofibrillar microenvironments (Wallimann et al., 1992). A corollary of our results suggests that whatever the specific functional roles for localization and organization of CK isoenzymes are, they are more subtle than those required in transporting the majority of energy equivalents within the cell or maintaining pools of cellular high-energy phosphates. Our results do not describe or depend on the details of the mitochondrial CK isoform, for which there appears to be a very significant degree of order and coupling of sMi-CK isoform with the adenine nucleotide transporter (Aliev and Saks, 1993; Wallimann et al., 1992).

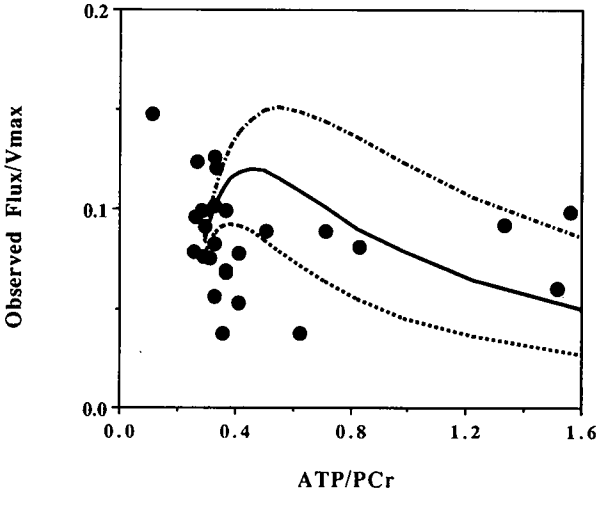

FIGURE 8 Comparison of observed (●; data as in Fig. 6) and predicted CK forward flux. The curves superimposed represent simulations of the effects of the anion-stabilized dead-end complex defined in the text (E·anion·Cr·MgADP). For these simulations, [anion] = [Cl^-] + [HCO_3^-] = 26 mM. The three curves represent, from top to bottom, KIi = 0.4, 0.2, and 0.1 mM (constant defined in text and Table 4).

SUMMARY

The data presented provide a detailed analysis of the behavior of the CK-catalyzed reaction in the soleus muscle in experiments designed to test three hypotheses: 1) the CK reaction is maintained near equilibrium with its substrates and products, both at rest and at different ATPase rates achieved by steady state stimulation; 2) the chemical flux through the CK reaction is independent of, and at least several times greater than, the ATPase and ATP synthesis rates (the latter two must be equal in the steady state); and 3) the in vivo flux is predicted from the in vitro enzyme kinetic constants and the observed substrate and product concentrations. The results cannot disprove the first or second hypothesis. Thus the creatine kinase reaction acts to maintain concentrations of ATP and ADP during metabolic transients as predicted by Eq. 1. The data provide no evidence for an obligate role in transport of high-energy phosphate between the site of synthesis (mitochondria) and utilization (myofibril). Predictions based on

obligatory shuttle function for creatine kinase predict increased flux when ATPase increases, and this was not observed. Tests of the third hypothesis yielded a surprising result, that the in vivo CK flux, 2.7 $mM \cdot s^{-1}$, was about 10-fold lower that expected from enzyme activity assays in vitro. The existence of the quaternary dead-end complex, E·anion·Cr·MgADP, present in the cytoplasm where chloride and bicarbonate are relevant anions, was sufficient to explain the difference. Thus the creatine kinase fluxes in cat soleus muscle are in fact predicted by conventional enzymology provided all of the relevant forms of the enzyme-substrate-product complexes are taken in to account.

We thank Leo Neuringer and the staff of the National Magnet Laboratory at the Massachusetts of Technology supported by grant RR 00995.
This work was supported by the Department of Radiology at the University of Washington and grants from the National Institutes of Health (R01AR36281 and R01AR38782 to MJK and F32 AR07762 to TSM).

REFERENCES

Alger, J. R., and R. G. Shulman. 1984. NMR studies of enzymatic rates in vitro and in vivo by magnetization transfer. *Q. Rev. Biophys.* 17:83–124.

Aliev, M. K., and V. A. Saks. 1993. Quantitative analysis of the "phosphocreatine shuttle": I. A probability approach to the description of phosphocreatine production in the coupled creatine kinate-ATP/ADP translocase-oxidative phosphorylation reactions in heart mitochondria. *Biochim. Biophys. Acta.* 1143:291–300.

Ariano, M. A., R. H. Armstrong, and V. R. Edgerton. 1973. Hindlimb muscle fiber populations of five mammals. *J. Histochem. Cytochem.* 21: 51–55.

Bessman, S. P., and P. J. Geiger. 1981. Transport of energy in muscle: the phosphorylcreatine shuttle. *Science.* 211:448–452.

Bittl, J. A., J. DeLayre, and J. S. Ingwall. 1987. Rate equation for creatine kinase predicts the in vivo reaction velocity: 31P NMR surface coil studies in brain, heart, and skeletal muscle of the living rat. *Biochemistry.* 26:6083–6090.

Bittl, J. A., and J. S. Ingwall. 1985. Reaction rates of creatine kinase and ATP synthesis in the isolated rat heart. *J. Biol. Chem.* 260:3512–3517.

Bittl, J. A., and J. S. Ingwall. 1987. Intracellular high-energy phophate transfer in normal and hypertrophied myocardium. *Circulation.* 75 (Suppl I):I-96–101.

Brindle, K. M., I. D. Campbell, and R. J. Simpson. 1987. NMR methods for studying enzyme kinetics in cells and tissue. *In* Biological Magnetic Resonance. L. J. Berliner and J. Reuben, editors. Plenum Press, New York.

Brindle, K. M., and G. K. Radda. 1987. 31P NMR saturation transfer measurements of exchange between Pi and ATP in the reactions catalysed by glyceraldehyde-3-phosphate dehydrogenase and phosphoglycerate kinase in vitro. *Biochim. Biophys. Acta.* 928:45–55.

Burke, R. E., D. N. Levine, M. Salcman, and P. Tsairis. 1974. Motor units in cat soleus muscle: physiological, histochemical, and morphological characteristics. *J. Physiol.* 238:503–514.

Campbell, I. D., C. M. Dobson, R. G. Ratcliffe, and R. J. P. Williams. 1978. Fourier transform NMR pulse methods for the measurement of slow-exchange rates. *J. Magn. Reson.* 29:397–417.

Conley, K. E., S. R. Kayar, K. Rosler, H. Hoppeler, E. R. Weibel, and C. R. Taylor. 1987. Adaptive variation in the mammalian respiratory system in relation to energetic demand: IV. Capillaries and their relationship to oxidative capacity. *Respir. Physiol.* 69:47–64.

Crow, M. T., and M. J. Kushmerick. 1982. Chemical energetics of slow- and fast-twitch muscles of the mouse. *J. Gen. Physiol.* 79:147–166.

Crow, M. T., and M. J. Kushmerick. 1983. Correlated reduction of velocity of shortening and the rate of energy utilization in mouse fast-twitch muscle during a continuous tetanus. *J. Gen. Physiol.* 82:703–720.

Degani, H., J. R. Alger, R. G. Shulman, O. A. C. Petroff, and J. W. Prichard. 1987. 31P magnetization transfer studies of creatine kinase kinetics in living rabbit brain. *Magn. Reson. Med.* 5:1–12.

Dulhunty, A. F. 1977. The dependence of membrane potential on extracellular chloride concentration in mammalian skeletal muscle fibers. *J. Physiol.* 276:67–82.

Forsen, S., and R. A. Hoffman. 1963. Study of moderately rapid chemical exchange reactions by means of nuclear magnetic double resonance. *J. Chem. Phys.* 39:2892–2901.

Forsen, S., and R. A. Hoffman. 1964. Exchange rates by nuclear magnetic multiple resonance. III. Exchange reactions in systems with several non-equivalent sites. *J. Chem. Phys.* 40:1189–1196.

Funk, C. I., A. J. Clark, and R. J. Connett. 1990. A simple model of aerobic metabolism: applications to work transitions in muscle. *Am. J. Physiol.* 258:C995-C1005.

Hoerter, J. A., C. Lauer, G. Vassort, and M. Gueron. 1988. Sustained function of normoxic hearts depleted in ATP and phosphocreatine: a ^{31}P-NMR study. *Am. J. Physiol.* 255:C192-C201.

Hoppeler, H. 1990. The different relationship of VO_2 max to muscle mitochondria in humans and quadrupedal animals. *Respir. Physiol.* 80: 137–146.

Hoppeler, H., O. Hudlicka, and E. Uhlmann. 1987. Relationship between mitochondria and oxygen consumption in isolated muscle. *J. Physiol.* 385:661–675.

Hore, P. J. 1983. Solvent suppression in Fourier transform nuclear magnetic resonance. *J. Magn. Reson.* 55:283–300.

Jacobus, W. E. 1980. Myocardial energy transport: current concepts of the problem. *In* Heart Creatine Kinase. W. E. Jacobus and J. S. Ingwall, editors. Williams & Wilkins, Baltimore.

Jacobus, W. E. 1985. Respiratory control and the integration of heart high-energy phosphate metabolism by mitochondrial creatine kinase. *Annu. Rev. Physiol.* 47:707–725.

Khalifah, R. G. 1971. The carbon dioxide hydration activity of carbonic anhydrase. *J. Biol. Chem.* 216:2561–2573.

Kupriyanov, V. V., A. Y. Steinschneider, E. K. Ruuge, V. I. Kapel'ko, M. Y. Dueva, V. L. Lakomkin, V. N. Smirnov, and V. A. Saks. 1984. Regulation of energy flux through the creatine kinase reaction in vitro and in perfused rat heart. *Biochim. Biophys. Acta.* 805:319–331.

Kushmerick, M. J., P. F. Dillon, R. A. Meyer, T. R. Brown, J. M. Krisanda, and H. L. Sweeney. 1986. 31P NMR spectroscopy, chemical analysis and free Mg^{2+} of rabbit bladder and uterine smooth muscle. *J. Biol. Chem.* 261:14420–14429.

Kushmerick, M. J., R. A. Meyer, and T. R. Brown. 1992a. Regulation of oxygen consumption in fast- and slow-twitch muscle. *Am. J. Physiol.* 263:C598-C606.

Kushmerick, M. J., T. S. Moerland, and R. W. Wiseman. 1992b. Mammalian skeletal muscle fibers distinguished by contents of phosphocreatine, ATP, and Pi. *Proc. Natl. Acad. Sci. USA.* 89:7521–7525.

Le Rumeur, E., L. Le Moyec, and J. D. De Certaines. 1992. Creatine kinase activity in rat skeletal muscle with intermittent tetanic stimulation. *Magn. Reson. Med.* 24:335–342.

McAuliffe, J. J., S. B. Perry, E. E. Brooks, and J. S. Ingwall. 1991. Kinetics of the creatine kinase reaction in neonatal rabbit heart: an empirical analysis of the rate equation. *Biochemistry.* 30:2585–2593.

McConnell, H. M. 1957. Reaction rates by nuclear magnetic resonance. *J. Chem. Phys.* 26:430–431.

McConnell, H. M., and D. D. Thompson. 1957. Molecular transfer of non-equilibrium nuclear spin magnetization. *J. Chem. Phys.* 26:958–959.

McFarland, E. W., L. J. Neuringer, and M. J. Kushmerick. 1988. Chemical exchange magnetic resonance imaging (CHEMI). *Magn. Reson. Imaging.* 6:507–515.

Meyer, R., M. Kushmerick, and T. Brown. 1982. Application of ^{31}P-NMR spectroscopy to the study of striated muscle metabolism. *Am. J. Physiol.* 242:C1-C11.

Meyer, R. A. 1989. Linear dependence of muscle phosphocreatine kinetics on total creatine content. *Am. J. Physiol.* 257:C1149-C1157.

Meyer, R. A., T. R. Brown, and M. J. Kushmerick. 1985. Phosphorus nuclear magnetic resonance of fast- and slow-twitch muscle. *Am. J. Physiol.* 248: C279-C287.

Meyer, R. A., H. L. Sweeney, and M. J. Kushmerick. 1984. A simple analysis of the "phosphocreatine shuttle." *Am. J. Physiol.* 246:C365-C377.

Moreadith, R. W., and W. E. Jacobus. 1982. Creatine kinase of heart mitochondria. *J. Biol. Chem.* 257:899–905.

Morrison, J. F., and W. W. Cleland. 1966. Isotope exchange studies of the mechanism of the reaction catalyzed by adenosine triphosphate: creatine phosphotransferase. *J. Biol. Chem.* 241:673–683.

Nunnally, R. L., and D. P. Hollis. 1979. Adenosine triphosphate compartmentation in living hearts: a phosphorus nuclear magnetic resonance saturation transfer study. *Biochemistry.* 18:3642–3646.

Roos, A. 1971. Intracellular pH and buffering power of rat muscle. *Am. J. Physiol.* 221:182–188.

Saks, V. A., G. B. Chernousova, D. E. Gukovsky, V. N. Smirnov, and E. I. Chazov. 1975. Studies of energy transport in heart cells—mitochondrial isoenzyme of creatine phosphokinase: kinetic properties and regulatory action of Mg2+ ions. *Eur. J. Biochem.* 57:273–290.

Sanyal, G., and T. H. Maren. 1981. Thermodynamics of carbonic anhydrase catalysis. *J. Biol. Chem.* 256:608–612.

Schimerlik, M. L., and W. W. Cleland. 1973. Inhibition of creatine kinase by chromium nucleotides. *J. Biol. Chem.* 248:8418–8423.

Schlegel, J. o., M. Wyss, U. Schurch, T. Schnyder, A. Question, G. Wegmann, H. M. Eppenberger, and T. Wallimann. 1988. Mitochondrial creatine kinase from cardiac muscle and brain are two distinct isoenzymes but both form octameric molecules. *J. Biol. Chem.* 263: 16963–16969.

Shoubridge, E. A., J. L. Bland, and G. K. Radda. 1984. Regulation of creatine kinase during steady state isometric twitch contraction in rat skeletal muscle. *Biochim. Biophys. Acta.* 805:72–78.

Ugurbil, K. 1985. Magnetization-transfer measurements of individual rate constants in the presence of multiple reactions. *J. Magn. Reson.* 64: 207–219.

Ugurbil, K., M. Petein, R. Maidan, S. Michurski, and A. H. L. From. 1986.Measurement of an individual rate constant in the presence of multiple exchanges: application to myocardial creatine kinase reaction. *Biochemistry.* 25:100–107.

Van Deursen, J., A. Heerschap, F. Oerlemans, W. Ruitenbeek, P. Jap, H. Ter Laak, and B. Wieringa. 1993. Skeletal muscles of mice deficient in muscle creatine kinase lack burst activity. *Cell.* 74:621–631.

Wallimann, T., M. Wyss, D. Brdiczka, K. Nicolay, and H. M. Eppenberger. 1992. Intracellular compartmentation, structure and function of creatine kinase isoenzymes in tissues with high and fluctuating energy demands: the "phosphocreatine circuit" for cellular energy homeostasis. *Biochem. J.* 281:21–40.

Watts, D. C. 1967. Creatine kinase (adenosine 5′-triphosphate-creatine phosphotransferase. *In* The Enzymes. P. D. Boyer, editor. Academic Press, New York.

Zahler, R., J. A. Bittl, and J. S. Ingwall. 1987. Analysis of compartmentation of ATP in skeletal and cardiac muscle using 31P nuclear magnetic resonance saturation transfer. *Biophys. J.* 51:883–893.

Zeleznikar, R. J., and N. D. Goldberg. 1991. Kinetic and compartmentation of energy metabolism in intact skeletal muscle determined from ^{18}O labeling of metabolite phosphoryls. *J. Biol. Chem.* 266:15110–15119.